P O L S K A   A K A D E M I A   N A U K
INSTYTUT MASZYN PRZEPŁYWOWYCH

PRACE INSTYTUTU MASZYN PRZEPŁYWOWYCH

TRANSACTIONS OF THE INSTITUTE OF FLUID-FLOW MACHINERY

70-72

WARSZAWA–POZNAŃ 1976

PAŃSTWOWE WYDAWNICTWO NAUKOWE

PRACE INSTYTUTU MASZYN PRZEPŁYWOWYCH

poświęcone są publikacjom naukowym z zakresu teorii i badań doświadczalnych w dziedzinie mechaniki i termodynamiki przepływów, ze szczególnym uwzględnieniem problematyki maszyn przepływowych

*

THE TRANSACTIONS OF THE INSTITUTE OF FLUID-FLOW MACHINERY

exist for the publication of theoretical and experimental investigations of all aspects of the mechanics and thermodynamics of fluid-flow with special reference to fluid-flow machinery

REDAKCJA – EDITORIAL OFFICE
Instytut Maszyn Przepływowych PAN
ul. Gen. Józefa Fiszera 14, 80-952 Gdańsk, skr. pocztowa 621, tel. 41-12-71

Printed in Poland

PAŃSTWOWE WYDAWNICTWO NAUKOWE – ODDZIAŁ W POZNANIU

Wydanie I. Nakład 630+90 egz. Ark. wyd. 63,25 Ark. druk. 49,25 Papier druk. sat. kl. V. 65 g., 70×100. Oddano do składania 4 VII 1975 r. Podpisano do druku w czerwcu 1976 r. Druk ukończono w czerwcu 1976 r. Zam. 528/118. H-16/245.
Cena zł 190,–

DRUKARNIA UNIWERSYTETU IM. ADAMA MICKIEWICZA W POZNANIU

III KONFERENCJA NAUKOWA

na temat

TURBINY PAROWE WIELKIEJ MOCY

Gdańsk, 24 - 27 września 1974 r.

*

IIIrd SCIENTIFIC CONFERENCE

on

STEAM TURBINES OF GREAT OUTPUT

Gdańsk, September 24 - 27, 1974

*

III НАУЧНАЯ КОНФЕРЕНЦИЯ

на тему

ПАРОВЫЕ ТУРБИНЫ БОЛЬШОЙ МОЩНОСТИ

Гданьск, 24 - 27 сентября 1974 г.

PRACE INSTYTUTU MASZYN PRZEPŁYWOWYCH
1976 Zeszyt 70 - 72

F. G. HAMMITT, LINH DO, G. C. ERNST, F. G. HAMMITT, JR., Y. C. HUANG, J. B. HWANG, A. KELLER, E. E. TIMM

U.S.A.*

Liquid-Induced Erosion Research

1. Introduction

The Cavitation and Multiphase Flow Laboratory of the Mechanical Engineering Department at the University of Michigan has been engaged for several years on a broad study of liquid-induced erosion and related problems from the viewpoint of both cavitation and liquid impact. It is the purpose of the present document to summarize briefly this work up to the present.

The erosion work is both experimental and theoretical. Experimental erosion studies involve several damage test facilities as well as ultra-high-speed photographic equipment:

1) high-speed cavitating water tunnel – to $\sim$65 m/s,

2) vibratory cavitation facility for a wide range of temperatures and pressures with almost any fluid including liquid metals as sodium,

3) rotating propeller arm device (4 ft. radius) for velocities to $\sim$550 m/s at pressures from 1/2 to 1 atm,

4) repeating water-gun facility producing elongated water slugs of $\sim$1.2 mm diameter with velocity to $\sim$600 m/s at repetition rate of $\sim$50 slugs/min.

In addition the following major experimental facilities, not erosion-producing, are in use:

1. Low pressure wet steam tunnel** for study of wet steam flows under vacuum and velocity conditions pertinent to the low pressure end of large steam turbines. The study includes the build-up and fragmentation of liquid films upon blading profiles inserted into a transparent test section. Test section conditions so far attained include pressure of 2 – 3 psia, and velocity close to Mach 1.

2. Bubble nucleation facility for study of bubble nucleation thresholds in various fluids (including sodium) as function of entrained gas microbubble population spectrum, imposed pressure wave frequency and amplitude, liquid temperature, etc. This work will not be discussed in further detail here, since it is not as closely related to the subject of the conference as the other studies.

The theoretical erosion work has concentrated upon computerized numerical studies of both collapsing cavitation bubbles ([1], e.g.) and individual droplet impacts upon flat

* The University of Michigan, Ann Arbor.

** Designed by Dr. J. Krzyżanowski of IMP PAN, Gdańsk, during his recent stay in our laboratory.

surfaces ([2], e.g.). Initially a non-deforming surface was considered, but in our presently on-going work, the surface deforms [3].

The present paper concerns itself primarily with our most recent erosion results (those from the water gun device), as well as initial results from the wet steam tunnel.

2. Water gun and droplet impact studies

2.1. Facility description

Though described elsewhere ([4], e.g.), the salient features are summarized here. The gun is a device using momentum exchange between an impacting spring-driven steel bolt and the impacting liquid. The momentum is transferred through a relatively stiff, but deflecting steel diaphragm. It is patterned after a device developed earlier by P. Kenyon [5], but somewhat modified for our present purposes.

Figure 1 is a schematic of the working section. A conical chamber formed in a steel plate is sealed on the back with a relatively thick steel diaphragm, struck by the steel bolt which is itself propelled by a heavy spring. Velocity is adjustable over the range 300–600 m/s, and repetition rates from 5–110/min. are possible.

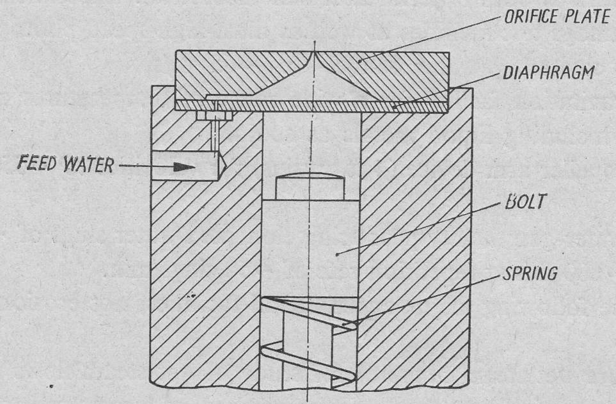

Fig. 1. Gun schematic

A photocell arrangement is used to set and monitor jet velocity. Typical jets at 3 velocities are shown in Fig. 2, indicating that the form of jet depends substantially upon velocity, so that the device is not well-suited to studying the general effect of impact velocity upon damage rate. Such results obtained with this device are then specialized to it.

2.2. Velocity effects upon damage

Figure 3 is a typical S-shaped erosion curve showing mean depth of penetration (volume loss/jet area) vs. height of impinging liquid column (assuming the impinging slugs to be reassembled into a single column), following the suggestion of Heymann for a recent liquid impact Round–Robin conducted in the U.S.A. by ASTM. The slope of the curve

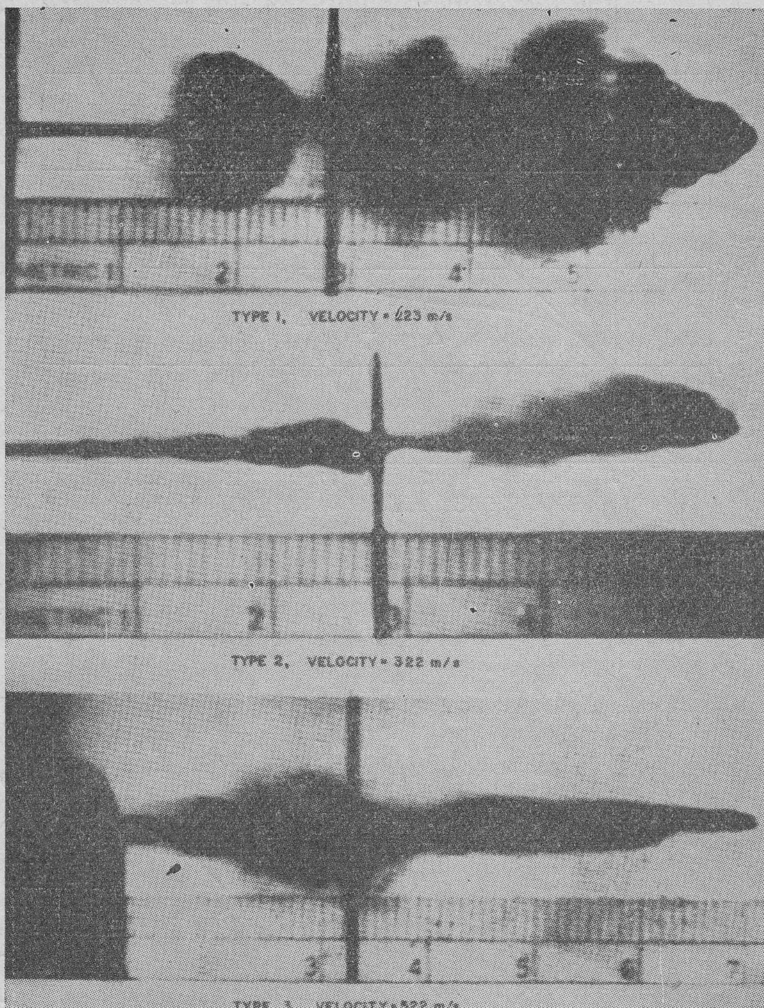

Fig. 2. Typical jets

is then a non-dimensional erosion rate, the ratio between depth of material removal and height of impacting liquid. The ratio is ~ 5000 in this case.

Figure 4 shows typical weight loss vs. number of impact curves at 400 and 600 m/s for soft aluminium (1100-0) and commercially pure nickel (270). Some material properties and test results are listed in Table. 1. The same results (smoothed curves) in terms of volume loss (proportional to mean depth of penetration) are shown in Fig. 5. From this data and also points at 480 m/s, the effect of velocity upon erosion rate is shown in Fig. 6, indicating a maximum damage velocity (~ 480 m/s) for this facility. It is of course unusual that the damage rate does not increase rapidly and continuously with increased velocity, but this unexpected result is apparently due to the change of jet shape with velocity (Fig. 2), previously discussed. The jet shape at high velocity is apparently relatively less damaging with this device than that produced at lower velocity.

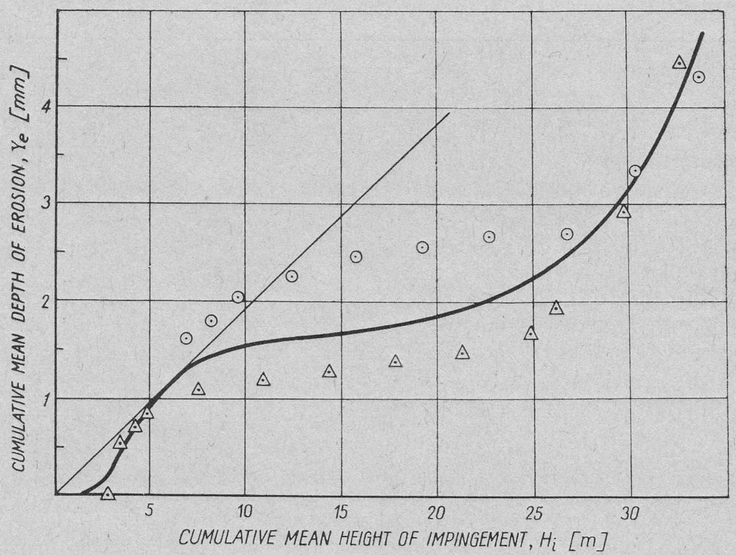

Fig. 3. Erosion curve of Plexiglas subjected to 400 m/s 90° impingement

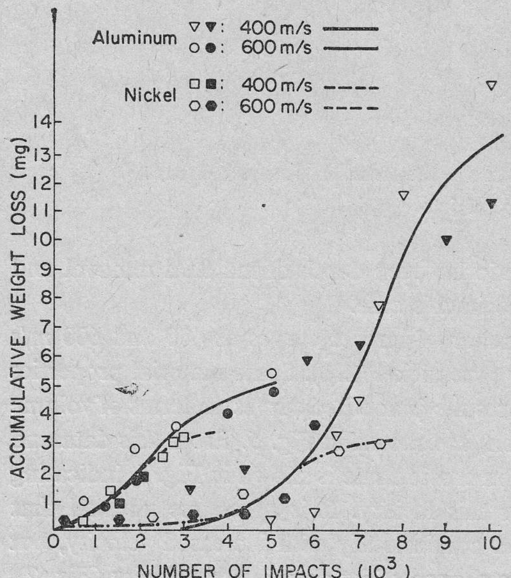

Fig. 4. Erosion curves of aluminum 1100-0 and nickel 270 subjected to 90° impingement

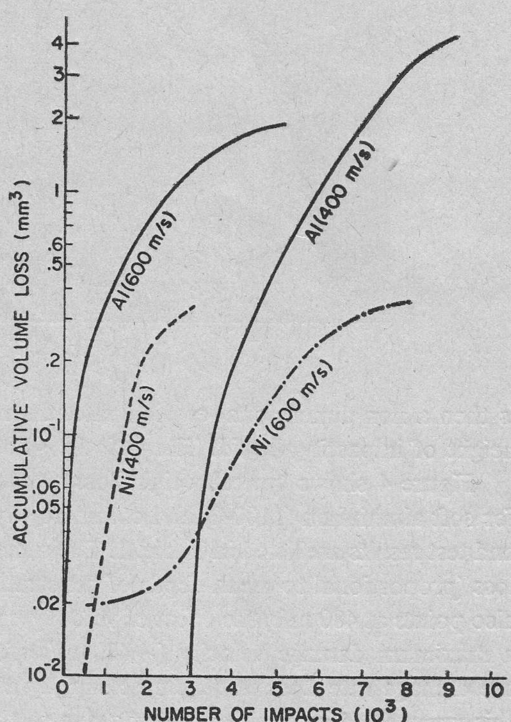

Fig. 5. Comparison between the volume loss of aluminum 1100-0 and nickel 270

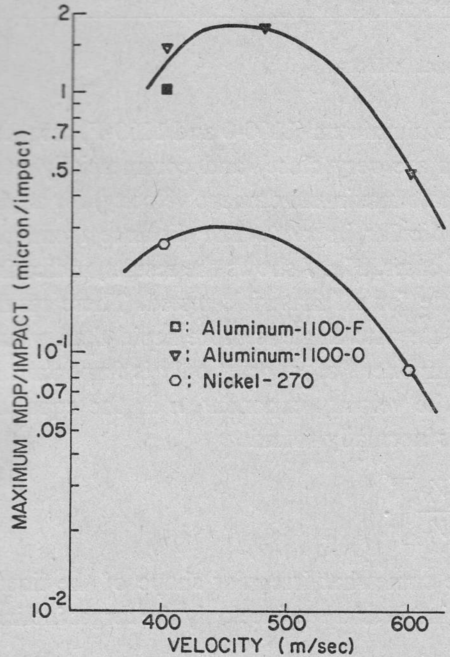

Fig. 6. Effect of impact velocity on maximum MDP rate (90° tests)

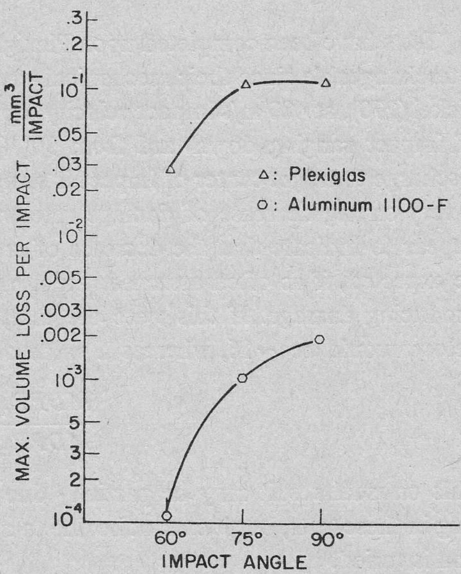

Fig. 7. Maximum volume loss/impingement vs. angle for Plexiglas and aluminum 1100-F

Table 1

Summary of test conditions and results

Specimen	Material	Test speed [m/s]	Test angle	Surface roughness (rms) [μm]	Rockwell hardness	Equivalent Brinell hardness	Maximum *MDPR**
1100-1	Aluminum 1100-0	400	90°	0.87	RE 28		1.45
1100-2				0.62	RE 25		
1100-4		600	90°	0.75	RE 25		0.49
1100-5				0.75	RE 29		
N-1	Pure Nickel 270	400	90°	1.25	RB 46	80	0.26
N-2				0.89	RB 40	75	
N-4		600	90°	1.25	RB 32	69	0.08
N-5				0.47	RB 30	67	
N-6				0.47	RB 30	67	
1100-5F	Aluminum 1100-F	480	90°	0.75	RE 31		1.72
1100-4F		480	60°	0.5	RE 30		0.19
1100-8F				0.75	RE 28		
1100-7F		480	30°	0.6	RE 33		0.0
1100-13F		480	45°	0.7	RE 34		0.0
1100-21F	Aluminum 1100-F	480	90°	0.6	RE 31		2.3
1100-22F				0.37	RE 32.5		
1100-23F			75°	0.38	RE 32		1.29
1100-24F				0.35	RE 35		
1100-25F			60°	0.36	RE 32		0.138
1100-26F				0.40	RE 33		
PLX-1, 2	Plexiglas	480	90°	–	–		153
PLX-3, 4			75°	–	–		153
PLX-5, 6			60°	–	–		34.4

* Rate of *MDP* change with respect to number of impacts.

2.3. Angle of impact effects

Tests have been completed upon Plexiglas, soft aluminum (1100-0 and 1100-F, assumed interchangeable since their mechanical properties are very close) and commercially pure nickel (270), at 480 m/s impact velocity (approximate maximum damage velocity) for angles of impact ranging downward from 90° (perpendicular impact). The distance from gun discharge to target center of impact is same in all cases. Fig. 7 shows the results, indicating a very strong decrease of damage rate with angle for all materials tested. These results appear to indicate that the decrease of erosion rate with angle is more rapid than would be expected, if as often assumed, the normal component of velocity only is important in producing damage. If this were the case, then the velocity exponent, n in the equation below, would be ~ 16, whereas a value of 5–6 is normally found

$$\frac{MDPR_{\max_1}}{MDPR_{\max_2}} = \left[\frac{V_{N_1}}{V_{N_2}}\right]^n.$$

This unusual result may be partially due to the somewhat irregular shape of the liquid slug in these tests, but it cannot be due to a changing jet shape, since only the target inclination is varied.

2.4. Impacts on resilient surfaces

A photographic investigation of splash impact patterns upon surfaces of differing resiliency is reported in detail elsewhere [6], and hence only summarized here. Perpendicular impacts at 223 m/s (500 MPH) upon Plexiglas and various elastomeric coatings (~ 0.84 mm) upon steel backing (~ 6 mm) have been conducted. Though there was little axial splash for a relatively non-deforming material such as Plexiglas (Fig. 8), there was considerable axial splash for some of the elastomerics (Fig. 9, e.g., for a grade of Neoprene). Natural rubber Fig. 10, on the other hand, showed little splash-back, being similar to Plexiglas in this respect. Thus at times the splash pattern differed considerably between apparently similar materials so that no meaningful correlation between splash pattern and erosion resistance as measured by the water gun, or other measured material properties, was found.

2.5. Theoretical studies

While our past numerical studies of droplet impact upon material surfaces has considered in general only non-deforming flat surfaces [7, 2], we are now extending this work to include surfaces exhibiting some resiliency. Two mathematical models have been studied.

2.5.1. Zero strength, inertial material model

Initial results were obtained [8] for the above material model, which is particularly pertinent for a soft elastomeric material. Impact of a spherical water drop at 270 m/s was studied for this case (Fig. 11). The considerable surface deformations shown indicate

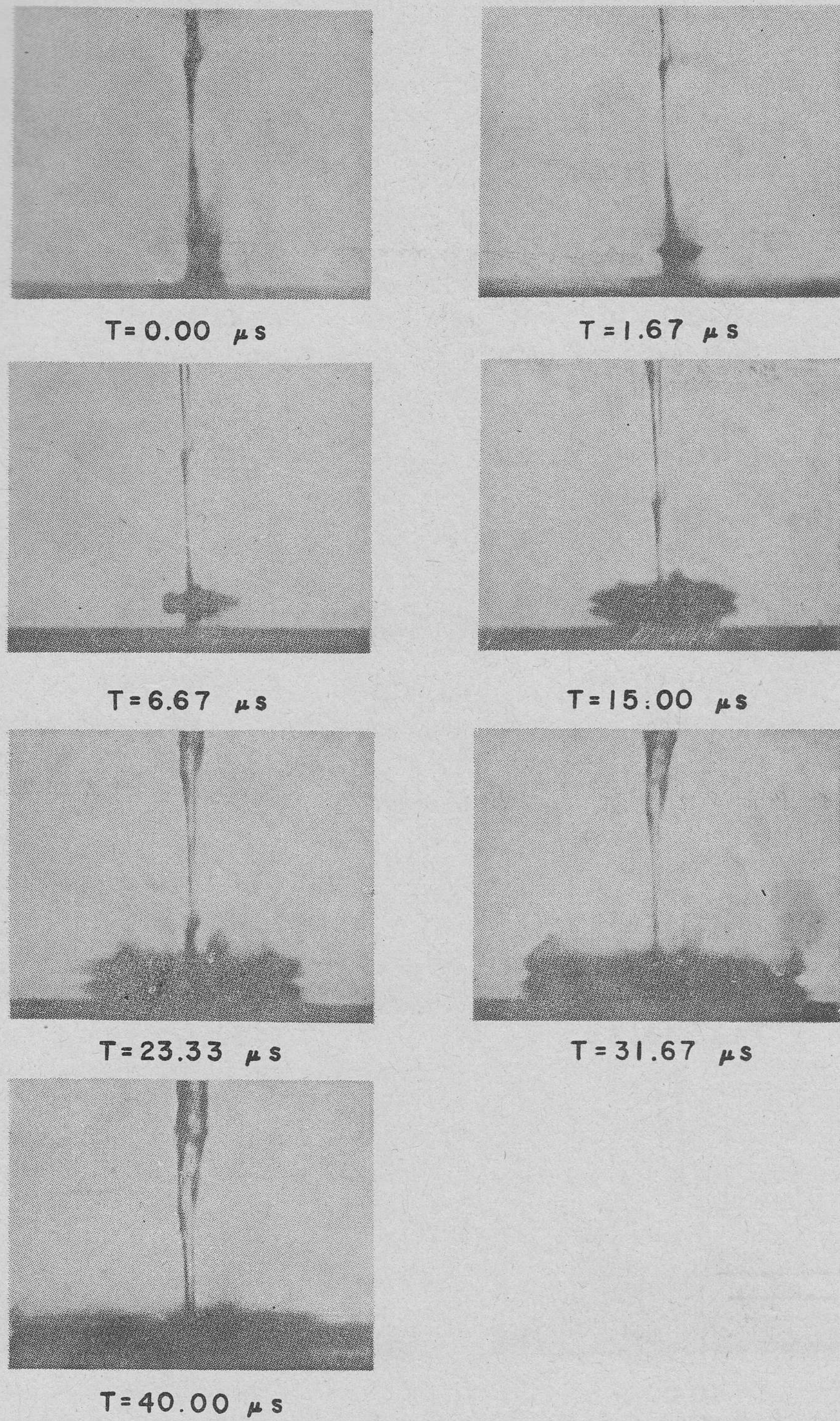

Fig. 8. High-speed motion picture sequence of jet impact – Plexiglas

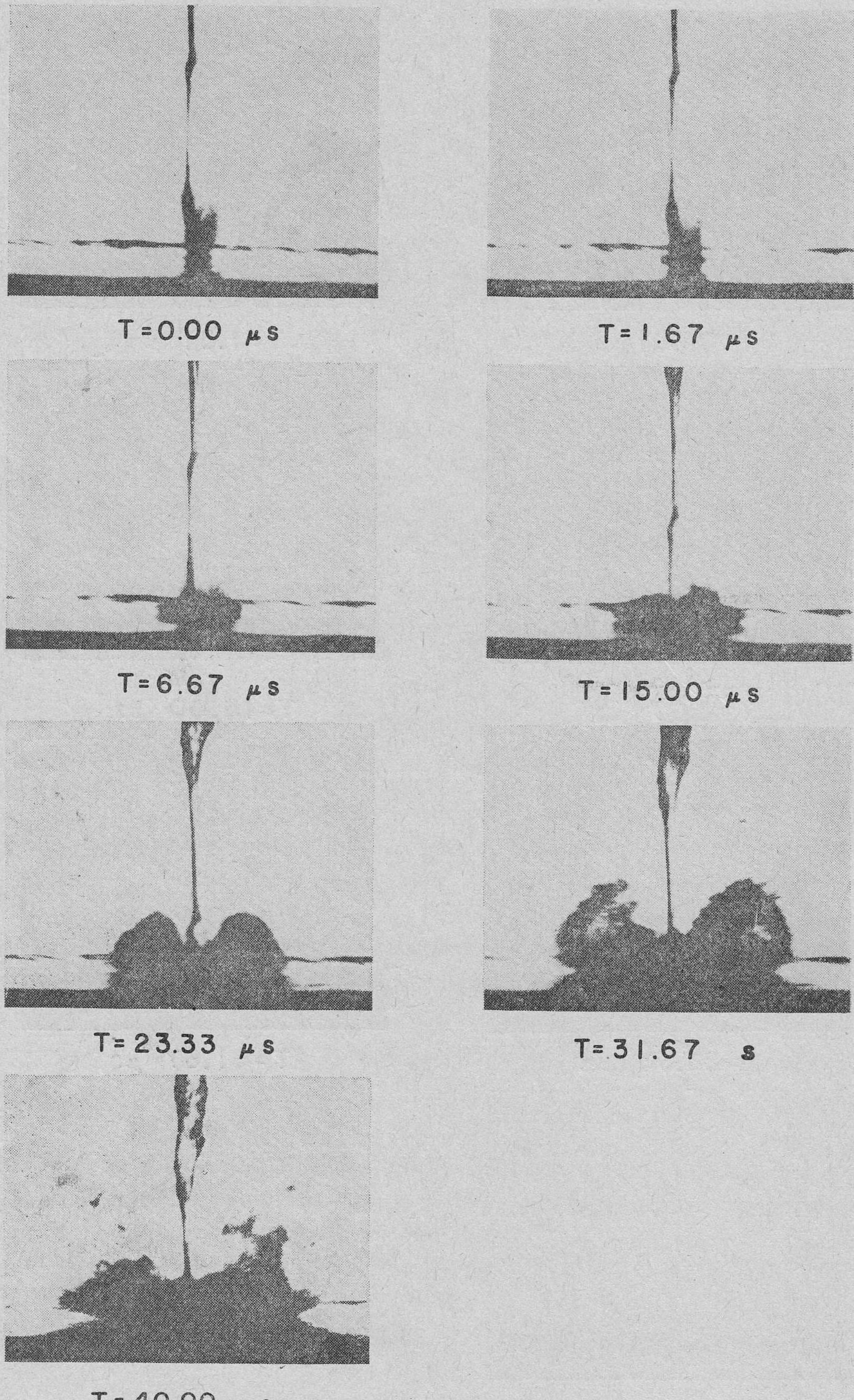

Fig. 9. High-speed motion picture sequence of jet impact – Goodrich #10

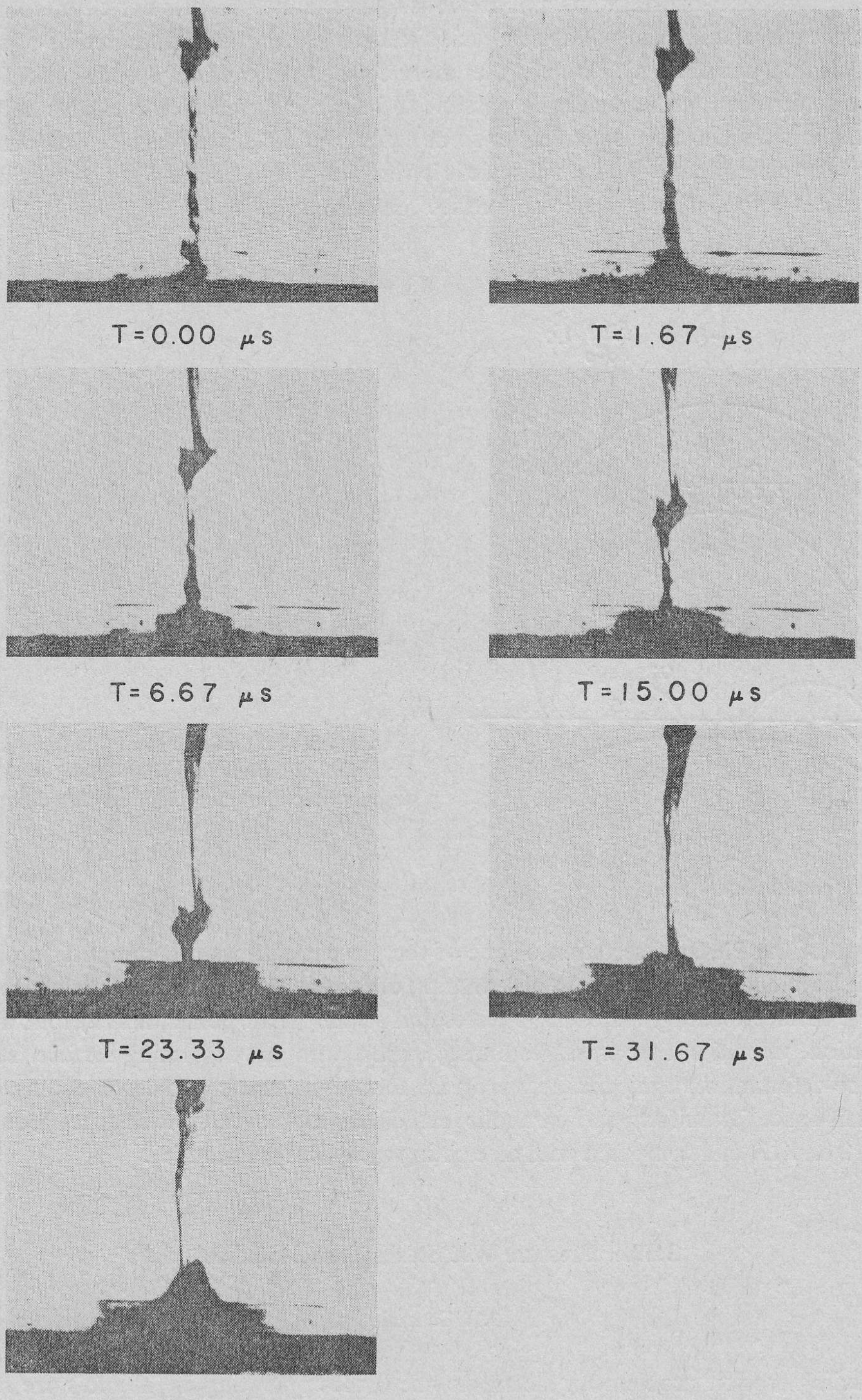

Fig. 10. High-speed motion picture sequence of jet impact – Goodrich #1 (natural rubber)

the reason for splash-back as shown in previous figures. However, it is not clear from these calculations why the intensity of splash-back differs so greatly between materials of similar elasticity (Fig. 9 and 10, e.g.). From further more detailed study of our splash-back pictures than has so far been made, it may be possible to infer the surface deformations necessary to create the splash, and thus confirm to some extent our calculated surface deformations. Due to its extreme rapidity and small scale it is very difficult to obtain a good experimental measurement of the instantaneous surface deformation.

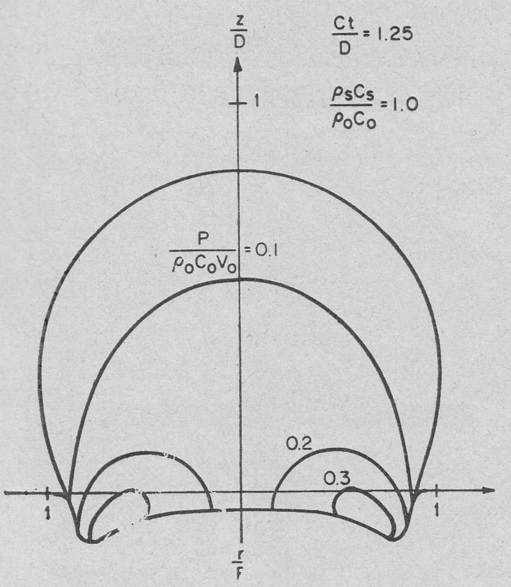

Fig. 11. Isobar distribution in an initially spherical droplet at time $Ct/D=1.25$, for impact Mach number of 0.2 on elastic boundary

2.5.2. Elastic material model

As part of the Ph.D. dissertation of one of the present authors [3], computer programs are being developed to 1) follow the deformation of an elastic solid material under arbitrary impulsive surface loading, indicating stresses and strains at all points, and 2) follow drop deformation, velocities, and pressures during impact with the deforming surface. Results of surface deformation using this new program for axisymmetric impulsive loading on an elastic half-space for uniform and parabolic load distribution over a circular area are shown in Fig. 12 and 13, and compared with an existing analytical solution [9].

3. Low Pressure Wet Steam Tunnel Studies

3.1. General

A blading erosion problem for steam turbine blades operating in the moisture regime has existed for many years. It has become more serious for present nuclear power plants, because of the low temperature steam provided, lacking usually in both superheat and reheat,

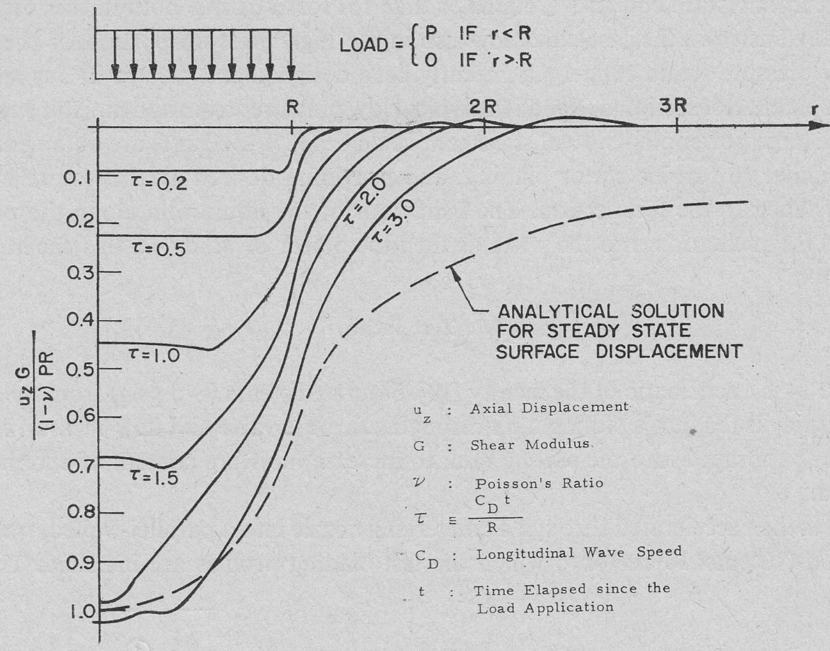

Fig. 12. Axial displacement on the surface of an elastic half-space due to the applications of uniform loading

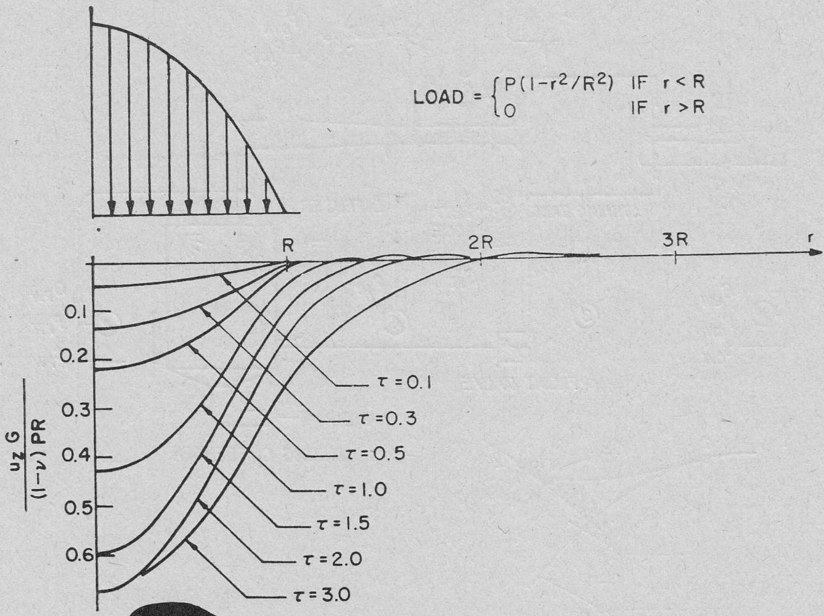

Fig. 13. Axial displacement on the surface of an elastic half-space due to the applications of parabolic loading

so that steam moisture contents are greater than for fossil plants, both in the low pressure end (as previously was the case), and now also in the high pressure portion of the turbine.

A low pressure steam tunnel has recently been designed and erected in our laboratory with transparent test section designed for typical low pressure steam and moisture conditions existing in large power plants. Realistic steam velocities (250–500 m/s) are obtained. Blading profiles similar to turbine stator blading, and providing desired axial pressure gradients, can be installed in the test section. The behaviour of the liquid film along the profile, as well as its fragmentation into the wake, is then the object of study in this facility, rather than erosion.

3.2. Test facility

Figure 14 is a schematic of the facility [10]. Saturated steam (~5 psig) from the building heating supply is fed into a stilling tank through a throttle valve and flow-measuring orifice. Water can be sprayed into the stilling tank to increase moisture content of entering steam as desired.

Steam is then accelerated through a converging nozzle into a parallel-walled, transparent test section (10 cm×10 cm) into which the test blading profiles are installed. The steam

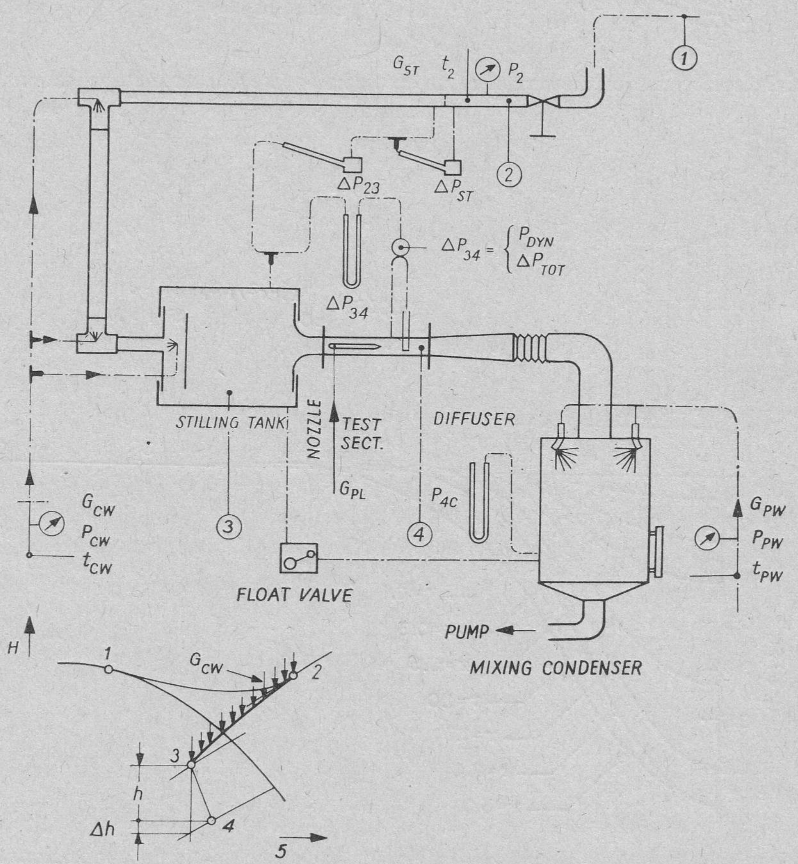

Fig. 14. Steam tunnel schematic

then traverses a diverging section, so that supersonic flow in the test section is possible, if the condenser vacuum is sufficient. A jet-type mixing condenser is used, into which a large quantity of cooling water is sprayed (about 50 × steam flow, which is ~14,00 lbm/hr max.). The condensed effluent is removed by a centrifugal pump into the sewer system, and air entrained with the steam is removed by a mechanical vacuum pump.

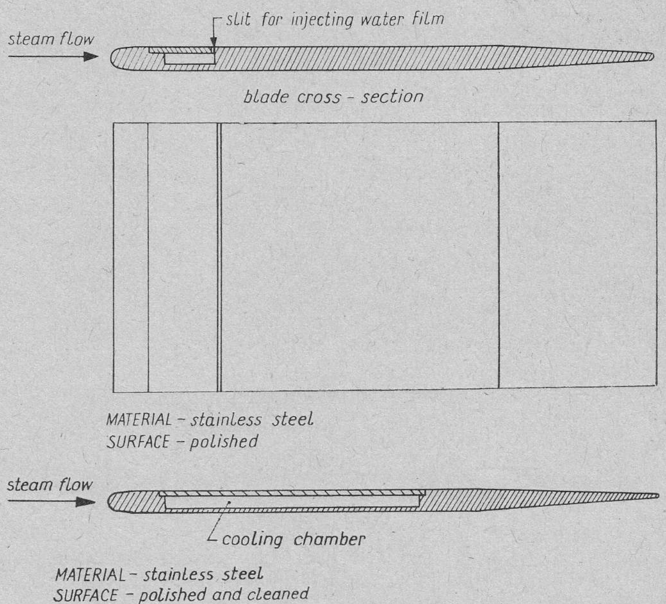

Fig. 15. a) Blade profile with injected water. b) Blade profile with internal cooling

Test section steam velocities are measured directly by Pitot tube traversed in the test section, and are calculated from an upstream orifice mass flow rate measure. At present, agreement between the methods is within ±15%, with Pitot providing the higher velocity. However, considering the uncertainties of impact tube data in two-phase flow, the orifice measure is probably more precise. Maximum test section velocity at present is ~1500 f/s, i.e., ~Mach 1.

Liquid films on the test profile can be induced either by direct injection of a water film along the profile boundary, or by internal water cooling of the profile (Fig. 15). The internally-cooled profile probably models more closely the liquid film formation in an actual turbine.

3.3. Preliminary test results

For the preliminary tests here described [11, 12], the symmetrical flat profile with tapered ends shown in Fig. 15 was used, with zero angle of attack. Photographic results were obtained both with injected water (Fig. 16), and with the blade internally-cooled (Fig. 17), providing a condensed film.

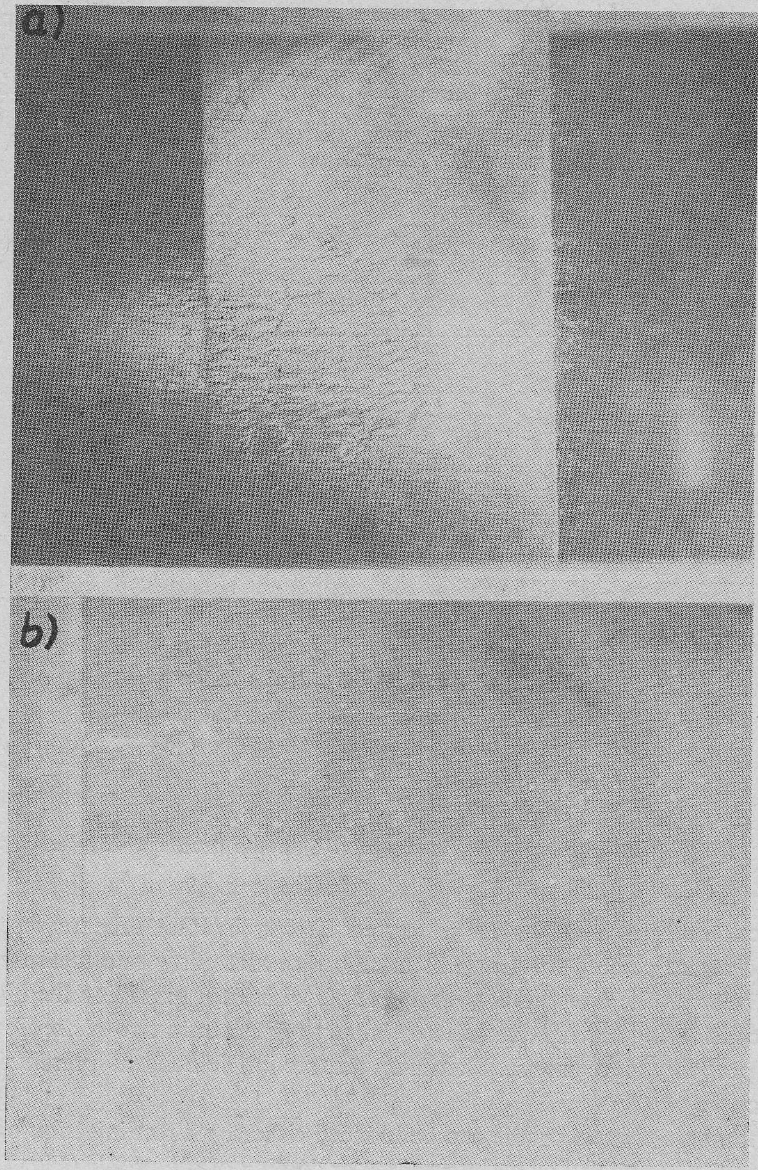

Fig. 16. Injected water film. Steam velocity: a) 437.8 m/s, b) 229.14 m/s. Film flow rate: a) 20 cc/min., b) 21 cc/min.

3.3.1. Injected water film (Fig. 16)

Fig. 16a shows surface waves a long the blade with the injected water film. These appear to originate at the point where the blade trailing edge (Fig. 15) begins. The surface wave at this point covers nearly the entire blade width.

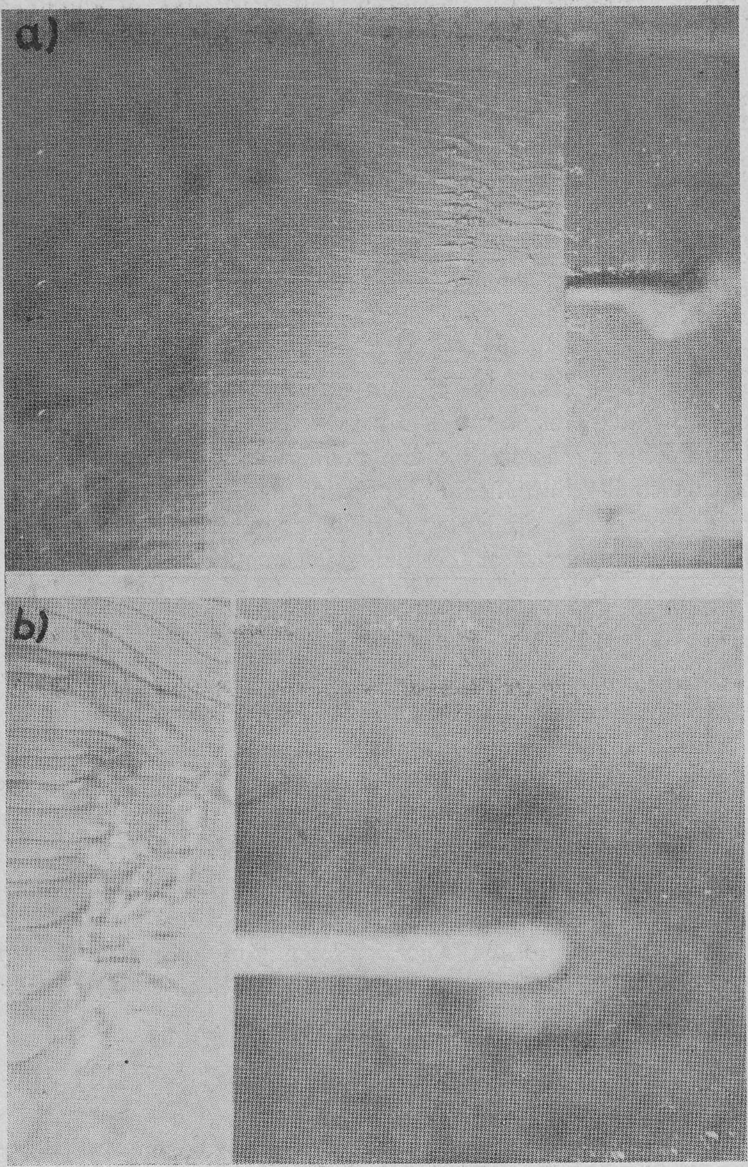

Fig. 17. Condensed water film. Steam velocity: 415 m/s. Film flow rate 120 cc/min.

Fig. 16b shows a tearing-off of the film in certain places, and the resultant droplet distribution in the steam-flow wake. The torn-off slug apparently does not separate into individual droplets until some distance downstream from the blade trailing edge. Before droplet formation, but after leaving the blade, the stream appears to twist into a vortex formation. The existence of a vortex at this point is also suggested by the angle of separation of the droplet paths after droplet formation. Droplet diameter in the wake is 0.05–0.1 mm.

3.3.2. Condensed water film (internally–cooled blade)

Fig. 17a shows the film streaming toward the trailing edge in fairly uniform fashion, and then fragmenting into droplets.

Fig. 17b shows the build-up of the condensed water film toward the blade trailing edge where it collects, eventually tearing-off under the action of the high-velocity steam into relatively large liquid slugs, which then pass downstream with the steam wake. The appearance of the film build-up at the trailing edge suggests that steam separation has occurred along this portion of the blade, due perhaps to an adverse pressure gradient along this tapered portion of the blade (Fig. 15). Thus there may be an upstream velocity component along the blade in this region, causing film build-up near the trailing edge, and generally retarding the breaking-off of film segments until relatively large slugs form, leading to an accelerated erosion problem when these impact the next moving blade row in an actual turbine. It is thus possible that modification of the blade shape in the region of the trailing edge could reduce the flow separation, and perhaps also the resultant droplet size in the wake. Thus further similar tests with differing blade profiles designed to evaluate the effect of pressure gradient near the trailing edge could be fruitful.

4. Conclusions

Various preliminary results concerning high velocity liquid droplet erosion of various metallic materials, and photographic details of the impact process and splash-back for various elastomeric materials, utilizing a water-gun device are presented. On the other hand, preliminary photographic observations of the behaviour of liquid films condensed from high-velocity low-pressure wet steam flowing past turbine blade profiles are also shown. In all cases the results are very preliminary, so that few firm general conclusions can be drawn at this point. These seemingly unrelated investigations are closely connected in motivation through droplet erosion, which is presently of considerable importance in the further development of very large steam turbines for the electric power industry.

References

[1] T. M. Mitchell and F. G. Hammitt, *Asymmetric Cavitation Bubble Collapse*. Trans. ASME., J. Fluids Engr., 95, 1, March 1973, 29 - 37.

[2] Y. C. Huang, F. G. Hammitt, W. J. Yang, *Hydrodynamic Phenomena During High-Speed Collision Between Liquid Droplet and Rigid Plane*. Trans. ASME, J. Fluids Engr., 1, 95, 2, 1973, 276-294; also available as ORA Report UMICH 01357-12-T (Mod. 2), Univ. Mich., Ann Arbor Michigan, August 1972.

[3] J. B. Hwang, *Liquid Impact on Elastic Materials*. Ph. D. Thesis Mechanical Engineering Department, University of Michigan, Ann Arbor, Mich.

[4] F. G. Hammitt, J. B. Hwang, Linh Do, F. G. Hammitt, Jr., Y. C. Huang, E. E. Timm, and R. D. Hughes, *Experimental and Theoretical Research on Liquid Droplet Impact*. To be presented at the Fourth Internation Conference, Meersburg, Federal German Republic, May 8–10. 1974; also available as ORA Report UMICH 01357-37 -T, Univ. Mich., Ann Arbor, Mich., February.

[5] H. F. Kenyon and P. H. Dawson, *Erosion by Water Jet Impacts, Part II – Characteristics of the Apparatus, and Part III – Erosion of a Turbine Blade Shield Material.* AEI Research Reports TP/R 5594 and 5626, 1967 and 1969.

[6] F. G. Hammitt, E. E. Timm, J. B. Hwang, Y. C. Huang, *Liquid Impact Behavior of Various Elastomeric Materials.* ASTM Committee G-2 Symposium, June, 1973; also available as ORA Report UMICH 01357-27-T, Univ. Mich., Ann Arbor, Mich., June 1973.

[7] Y. C. Huang, *Numerical Studies of Unsteady, Two-Dimensional Liquid Impact Phenomena.* Ph. D. Thesis, Mechanical Engineering Department, University of Michigan, Ann Arbor, Michigan, June 1971, ORA Report UMICH 03371-8-T.

[8] Y. C. Huang and F. G. Hammitt, *Liquid Impact on Elastic Solid Boundary.* Proc. 11th Radome Symp., Geo. Inst. Techn., July 1972; also available as ORA Report UMICH 03371-12-I, Univ. Mich., Ann Arbor, Mich and US Govt, Printing Office.

[9] G. Eason, *The Displacement Produced in an Elastic Half-Space by a Suddenly Applied Surface Force.* J. Inst. Math. and Applications, 2, 299-326, 1966.

[10] J. Krzyżanowski, *Wet-Steam Tunnel Facility — Design and Program of Investigations.* ORA Report No. UMICH 01357-18-T, Univ. Mich., Ann Arbor, Michigan, June 1972.

[11] F. G. Hammitt, A. Keller, G. A. Ernst, *Low -Pressure, Wet, Steam Tunnel – Initial Operation and Results.* ORA Report No. UMICH 012449-1-T, Univ. of Mich., Ann Arbor, Michigan, January 1974.

[12] F. G. Hammitt, A. Keller, G. A. Ernst, *Low-Pressure, Wet, Steam Tunnel — Initial Results.* Submitted for 1974 ASME Polyphase Flow Forum, May 1974; available as ORA Report No. UMICH 012449-1-I, January 1974.

Badanie erozji wywołanej działaniem cieczy

Streszczenie

Przedstawiono wyniki badań erozji materiałów metalicznych, prowadzonych przy użyciu urządzenia wyrzucającego strumień wody; wskazują one na zależność szybkości erozji od prędkości i kierunku padania strumienia. Pokazano, że dla użytego urządzenia istnieje prędkość odpowiadająca maksymalnej szybkości erozji. Pokazano również, że ze zmianą kąta padania uzyskano większą zmianę szybkości erozji niż można byłoby oczekiwać.

Przedstawiono sekwencje zdjęć uderzenia strumienia wykonanych szybkoobrotową kamerą filmową, dla różnych materiałów niemetalicznych. Zdjęcia ukazują szczegóły obserwowanych rozprysków. Mimo, że te ostatnie różnią się bardzo dla różnych materiałów, nie udało się znaleźć żadnej korelacji pomiędzy rozkładem rozprysków a odpornością na uderzenia strumienia lub innymi własnościami materiałów.

Zaprezentowano wstępne obserwacje fotograficzne fragmentacji i narastania filmu cieczowego na profilach odpowiadających profilom łopatek turbinowych w niskociśnieniowych przepływach mokrej pary wodnej. Okazuje się, że wielkość cząstek cieczy, pojawiających się później w śladzie aerodynamicznym, może zależeć silnie od osiowego gradientu ciśnienia w pobliżu krawędzi spływu łopatki. Minimalizacja i kontrola wielkości tych kropel jest oczywiście bardzo ważna dla minimalizacji powodowanej przez krople erozji następnego szeregu wirujących łopatek we współczesnej turbinie parowej dużej mocy.

Исследование эрозии вызванной действием жидкости

Резюме

Представлены результаты исследований эрозии металлических материалов, проведенных при помощи устройства выбрасывающего поток воды. Они указывают на зависимость скорости эрозии от скорости коллизии. Показано, что для данного устройства существует значение скорости потока,

которому отвечает максимальная скорость процесса эрозии. Это происходит вероятно за счет изменения формы фронта потока в функции его скорости. Для этого же самого устройства показано влияние угла атаки, указывая на более сильное, чем можно было бы ожидать, падение скорости эрозии ввиду изменения угла.

Представлены последовательные снимки удара потока в различные материалы, сделанные быстродействующей кинокамерой. На снимках видны подробности наблюдаемых форм разбрызгов. Мимо того, что эти последние очень различаются для разнообразных материалов, не удалось найти никакой корреляции между формой разбрызгов и прочностью против ударам потока или другими свойствами материалов.

Представлены результаты предварительных фотографических наблюдений образования и распада пленки жидкости на пластинках, моделирующих профиль турбинных лопаток в потоке влажного водяного пара при низких давлениях. Оказывается, что величина капель жидкости, появляющихся позднее в аэродинамическом следу, может сильно зависеть от аксиального градиента давления вблизи выходной кромки лопатки. Минимализация и контроль величины этих капель, конечно, оказываются очень важными с точки зрения ограничивания эрозии, вызываемой каплями в венцах рабочих лопаток современных паровых турбин большой мощности.